Auger parameters and screening mechanisms in the 4*d* and 5*d* metals

G. G. Kleiman, R. Landers, P. A. P. Nascente, and S. G. C. de Castro
Instituto de Física, Universidade Estadual de Campinas, 13081 Campinas, São Paulo, Brazil
(Received 5 September 1991)

We report measurements of $L_3M_{4,5}M_{4,5}$ Auger spectra for Nb, Mo, Ru, Rh, Pd, Ag, In, Sn, and Sb. Detailed calculations indicate that the spectra are well described by the intermediate-coupling scheme, as we illustrate for In. The notion that the core-hole states are completely relaxed implies that the Auger parameter is the sum of a slowly varying core term and a term that is sensitive to the valence-electron configuration but independent of the core-level identities, which seems to be borne out by the $L_3M_{4,5}M_{4,5}$ and $M_5N_{4,5}N_{4,5}$ Auger parameters. The theoretical systematics of a model involving the quasiatomic picture indicates that the valence-electron contribution to the Auger parameter can be isolated. Comparison of the $L_3M_{4,5}M_{4,5}$ and $M_5N_{4,5}N_{4,5}$ results is consistent with the idea that the *d*-band holes behave as core holes in the screening process. Furthermore, it appears that certain of the screening parameters can be extracted from the data, resulting in values in reasonable agreement with independent calculations and in good agreement with experiment. Calculations for the 5*d* series are in good agreement with experiment, and we illustrate the separate contributions to the Auger parameter and the influence of screening in this case.

I. INTRODUCTION

Interpretation of a number of x-ray photoelectron spectroscopy (XPS) and x-ray excited Auger electron spectroscopy (XAES) measurements in metals and alloys is impossible without understanding the corresponding excited electronic valence states. The simplest such excited state corresponds to what has been interpreted as a completely screened long-lived core hole[1] so that, in its final state, the system has relaxed to the "ground state" of neutral metal plus core hole.[2] In this relaxed state, the electronic valence-band properties, such as the local density of states, are self-consistently determined in the presence of the core hole.[3]

This picture of the relaxed state has been used to analyze XPS atom-metal binding energy shifts,[1,4] satellite positions,[5,6] and XAES features[5-8] through application of the quasiatomic model (QAM). Common versions[1,4-7] of the QAM usually treat the core hole as an extra proton (the "equivalent core" model[9-12]) and self-consistently add a valence electron to a $z+1$ impurity in a metal with atomic number z (corrections to the equivalent core model have been considered[8]).

XAES involves an initial core hole and a final two-hole state of the metal, so that it may be considered as an excited-state spectroscopy (we denote the valence band by V, and core levels by i, j, and k). In this context, it is interesting to examine the validity of the quasiatomic model of core-hole screening by investigating ξ, the final-state effective hole-hole Coulomb interaction, or Auger parameter, which is defined in Eq. (1). For an Auger transition involving levels i, j, and k,[7]

$$\xi_{ijk} \equiv (B_i - B_j - B_k) - K_{ijk} = B_j^{(k)} - B_j \ , \tag{1}$$

where B_j denotes the binding energy of level j in the ground state, $B_j^{(k)}$ is that when there is a hole in level k, and K_{ijk} represents the experimental Auger kinetic energy relative to the Fermi energy. The first equality in Eq. (1) presents ξ as the difference between the experimental Auger energy and that corresponding to uncorrelated holes, so that ξ is a measure of electron-electron interaction effects.

The QAM has been applied, with considerable success, to explain the systematics of ξ_{ijk} (i.e., core-level spectra) in the 3*d*,[7,13] the 4*d*,[14] and the 5*d* (Refs. 13 and 15) metal series: these systematics of ξ_{ijk} exhibit a monotonic increase with increasing z and a large jump between the Pt and noble-metal group metals, which is attributed to the change from *d*- to *s*-electron screening.

Auger parameters taken from iVV spectra of these metals[16-18] manifest similar systematics, which are correlated with the evolution of these spectra from bandlike to quasiatomic.[19] This correlation led to the common explanation that the line-shape evolution occurs because the screening charge of the valence-band *d* holes changes from *d* to *s* type. Furthermore, it was concluded that the final-state holes responsible for the $^1G_4$ term in Ni and Pd may be treated as core holes.[5,6,8] Such a conclusion is supported by studies of Ni,[5,19] Cu,[16,19] Zn,[16,20] Pd,[6] and Ag.[21]

The question of whether valence *d*-band holes are quasiatomic or are bandlike, or are some combination of the two is naturally of fundamental interest. Deriving the answer from Auger line shapes, however, is often not simple. For example, even though Pd in dilute Pd-Ag and Pd-Cu alloys is though to have no ground-state *d* holes, and the Pd $M_{4,5}VV$ spectra have been interpreted as arising from quasiatomic *d*-band hole states,[22-29] controversy has arisen regarding the interpretation[28,29] and the line shapes are sensitive to the alloy environment.[24-34]

The picture is less clear still for metals with multiple ground-state d-band holes. For example, interpretation[6] of the Pd $M_{4,5}VV$ spectrum as quasiatomic relies upon its incompatibility with the self-convoluted XPS valence-band spectrum. In addition, the spectrum peak energy was identified with the dominant $^1G_4$ final-state atomic multiplet term. Since even the admittedly quasiatomic Pd spectra[24–29] in Pd-Ag and Pd-Cu alloys are modified drastically by band effects, such as quasiatomic interpretation of the spectrum of Pd metal, however, is not necessarily valid.[30]

The application of XAES energy shifts to complement XPS information[3,35–38] and to extract thermochemical data[8,39] depends on the final-state holes being corelike. Since the iVV spectra are often the most convenient to measure, the validity of these applications of the energy shifts requires investigation of the nature of the final-state holes.

The QAM is a model of valence-electron screening of core holes. Investigation of the applicability of the QAM to *valence d-band* holes, therefore, would be facilitated by comparison with measurements of Auger transitions involving only core holes. In the 3d series, however, such core-level spectra are complex and broad[16] and the energy accuracy necessary for a sensible comparison is difficult to achieve experimentally.

The $L_{2,3}M_{4,5}M_{4,5}$ core-level spectra of the 4d series are sufficiently simple in form and narrow enough to permit determining the Auger parameter with the accuracy necessary, even though they are not commonly measured because of their high kinetic energy. In this paper, we present results of measurements of the $L_3M_{4,5}M_{4,5}$ spectra, and, although the emphasis is on deriving the corresponding Auger parameters, we display for In a comparison with the results of atomic calculations for this transition.

By comparing the Auger parameters derived from these data with the respective ones for the $M_5N_{4,5}N_{4,5}$ transitions[17] within the context of the QAM, we demonstrate the possibility of isolating the valence-electron contribution to ξ from the experimental data alone. Throughout, we pay careful attention to the hierarchy of approximations made, so that we can determine, for example, which results are consequences of the basic approximation of complete screening and which are artifacts of the model we employ. The principal conclusion of this study is that the valence-electron contributions to the Auger parameters of both the M_5VV and $L_3M_{4,5}M_{4,5}$ transitions agree within experimental error for most of the metals considered, supporting the treatment of valence d-band holes as corelike. A preliminary report of these findings was published elsewhere.[14]

In Sec. II of this paper, we describe the experimental techniques and results. We discuss these results in Sec. III and show that the theoretical systematics, which we motivate physically, allow separation and comparison of the valence-electron contributions to ξ_{MVV} and ξ_{LMM}. Theoretical predictions of the model are illustrated for the $M_4M_{6,7}N_{6,7}$ transition in the 5d series and compared, where possible, with independent results. We present our conclusions in Sec. IV.

II. EXPERIMENTAL RESULTS

We measured the $L_3M_{4,5}M_{4,5}$ core-level spectra of Nb, Mo, Ru, Rh, Pd, Ag, In, Sn, and Sb. All the samples were in the form of foils, except for Ru, which consisted of an electron beam evaporated film on a Pd substrate, and Sb, which was a crystal. The foils were polished to a mirror finish, except for the In and Sn samples, whose surfaces were mechanically scraped just before insertion in the analysis chamber. The samples were cleaned by Ar-ion sputtering before analysis and only amounts of oxygen so small that they were difficult to distinguish from the background were detected and then only on In, Sn, and Sb. The 3d spectra of all of the samples were measured and none manifested any effect of contamination at this point.

The high melting point metals were then annealed at 1000 K to reorder their surfaces and to remove impurities such as C and O. The spectroscopic measurements were performed using Al $K\alpha$ radiation (1486.6 eV) with a Vacuum Science Workshop (VSW) HA100 hemispherical analyzer (background pressure of 8×10^{-11} to 2×10^{-10} torr) in the fixed analyzer transmission (FAT) mode with a pass energy of 44.0 eV, which yielded a fullwidth at half maximum (FWHM) of 1.2 eV for the Au $4f_{7/2}$ peak. The energy scale of the spectrometer was calibrated relative to the Fermi level of the collector by precisely biasing a freshly sputtered Au sample in order to shift the kinetic energy of the $4f_{7/2}$ electrons (84.0 eV binding energy) to the energy range of interest. The Auger spectra were measured over 50.0-eV ranges in steps of 0.05 eV and were excited by bremsstrahlung excited Auger spectroscopy[40] (BEAS) with an Al anode (15.0-mA current at 12.0-kV voltage). Over the 50-eV energy ranges of interest, the correction for the analyzer's energy-dependent transmission (inversely proportional to the kinetic energy) was small, around 2% at most for Nb, where the correction was largest. Spectra are presented here with the inelastic background removed by subtracting a constant fraction of the intensity integrated to higher kinetic energies than that considered.[41]

The spectroscopic measurements of the $L_3M_{4,5}M_{4,5}$ spectra took typically from 12 to 18 hours to achieve adequate signal-to-noise ratios. During this time oxygen contamination was unavoidable. The effect of contamination was monitored by measuring the 3d and other sensitive XPS spectra. All the XPS peak energies and line shapes corresponded to literature values and we believe that the small amount of oxygen detected (e.g., around 2% for Mo) did not affect our measurements appreciably. This view is reinforced by the high kinetic energies of the XAES spectra (from around 2000.0 to 3000.0 eV), which correspond to electronic mean free paths on the order of 3.0 to 10.0 nm.[42]

The $L_3M_{4,5}M_{4,5}$ spectrum for In is displayed in Figs. 1(a) and 1(b). Although the states involved in the transition are the same as for the L_3VV spectra measured previously in the 3d series,[16] there are significant differences between the spectra. For example, two peaks appear on the high-energy side of the In main peak in Fig. 1, as opposed to one peak in the case of Ga.[16] These differences

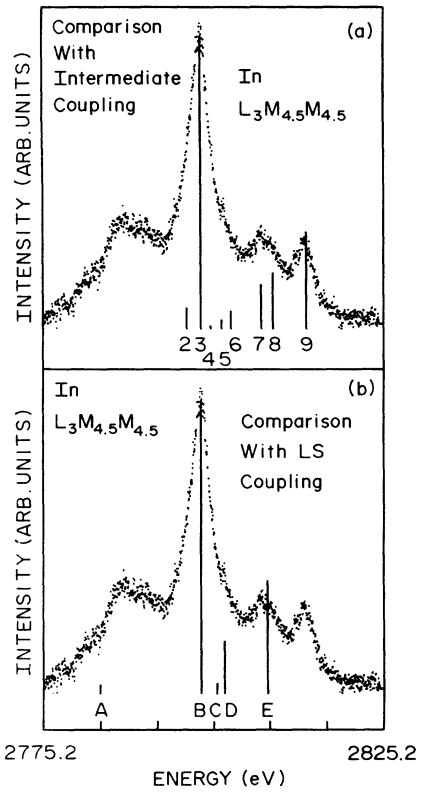

FIG. 1. (a) The measured $L_3M_{4,5}M_{4,5}$ spectrum for In compared with the results of intermediate-coupling calculations whose labels are identified in Table I. The $^1S_0$ in Table I has negligible intensity and is not shown. Details of the calculations and experimental $L_3M_{4,54}M_{4,5}$ spectra of other 4*d* metals are presented in Ref. 49. (b) The In spectrum of Fig. 1(a) compared to the results of *LS* calculations. Identification of the labels is given in the last column of Table I. This comparison is intended to exhibit the inadequacy of *jj-LS* calculations.

may be attributed to the applicability of the intermediate-coupling[43] (IC) description of the multiplet splittings of the experimental spectra in Figs. 1 as opposed to the *LS* coupling[43] description of the corresponding 3*d* spectra.[16]

This point is illustrated by the results of calculations represented by vertical lines in Fig. 1, where the most intense term was aligned with the largest experimental peak. In Fig. 1(a), the multiplet splittings were calculated within the intermediate, coupling scheme,[43] where the spin-orbit parameter[43] was derived from the XPS 3*d* splitting (i.e., $\zeta_{3d}=3.02$ eV) and the Slater integrals[44] were taken from Mann's tables.[45] The intensities were calculated in *jj* intermediate coupling[46,47] (*jj*-IC) using McGuire's integrals.[48] For purposes of comparison, Fig. 1(b) displays *LS* multiplet splitting[43] and *jj-LS* intensities.[47] Table I presents the identifications, intensities, and energy positions of the IC and *LS* terms in Fig. 1. Detailed expressions, and calculated spectra as well as energies and intensities of all the terms for all the metals considered here are given elsewhere.[49]

In Fig. 1(a), no attempt was made to optimize either the Slater integrals or any other calculational parameters. Under these circumstances, the agreement between theory and experiment is quite satisfactory. The structure at lower kinetic energies than that of the main peak appears to arise from plasmon losses, although other types of loss structure occur for 4*d* metals of lower z.[49]

We used the same procedure to calculate the Auger parameters for the $L_3M_{4,5}M_{4,5}$ transitions as that used previously[17] for the $M_5N_{4,5}N_{4,5}$ in order to be able to make a sensible comparison between them. Since this involves substituting twice the weighted mean binding energies of M_4 and M_5 [binding energies $B(M_4)$ and $B(M_5)$, respectively] for B_j+B_k in Eq. (1), the expression takes the form in Eq. (2).

$$\xi_{LMM}=[B(L_3)-B(M_5)]+\{[B(M_4)-B(M_5)]/5\}-B(M_4)-K_{LMM}\ . \quad (2)$$

Both the first and second terms in square brackets involve differences of binding energies, and, so, to minimize errors, we determine them from very accurate x-ray transition energies[50] (in practice, the XPS 3*d* splitting yields the second term with sufficient accuracy). The remaining

TABLE I. Identification of the calculated multiplet terms for In in Fig. 1. The first column associates the label in Fig. 1(a) with the corresponding eigenvector component in the limit of negligible spin-orbit coupling [in our intermediate-coupling (IC) calculations, the spin-orbit parameter, $\zeta_{3d}=3.01$ eV, from the XPS 3*d* splitting]. The second and third columns present the IC energies and *jj*-IC intensities relative to $^1G_4$ (absolute intensity 100.53×10^{-4} a.u.). The fourth and fifth columns display the *LS* energies and *jj-LS* intensities relative to $^1G_{44}$ (absolute intensity 111.71×10^{-4} a.u.), and the corresponding lettered labels in Fig. 1(b). Strongly mixed IC states are marked with an asterisk. Details are given in Ref. 49.

Term	IC energy	IC intensity	*LS* energy	*LS* intensity	
(1) $^1S_0$	−17.33	0.00	−14.77	0.03	*A*
(2) $^{*3}P_2$	−2.09	0.07	2.38	0.03	*C*
(3) $^1G_4$	0.00	1.00	0.00	1.00	*B*
(4) $^3P_1$	1.48	0.01	2.38	0.01	*C*
(5) $^3P_0$	3.13	0.03	2.38	0.00	*C*
(6) $^{*1}D_2$	4.50	0.06	3.53	0.17	*D*
(7) $^3F_3$	9.03	0.15	9.94	0.13	*E*
(8) $^{*3}F_2$	10.72	0.19	9.94	0.08	*E*
(9) $^3F_4$	15.68	0.33	9.94	0.20	*E*

TABLE II. Energies (in eV) employed in Eq. (2) for the $L_3M_{4,5}M_{4,5}$ Auger parameter, as discussed in the text. The L_3-M_5 x-ray energies and M_4 binding energies were taken from Refs. 50 and 52, respectively. The M_5VV Auger parameters were recalculated with the same M_4 binding energies.

Element	Auger energy	$3d$ splitting	ξ_{LMM}	ξ_{MVV}
Nb	1937.97	2.73	23.6	0.2
Mo	2038.29	3.13	24.5	0.7
Ru	2249.44	4.14	25.9	0.6
Rh	2358.49	4.70	27.4	0.5
Pd	2469.12	5.27	30.5	3.3
Ag	2576.91	5.99	34.4	4.9
Cd		6.74		5.9
In	2798.34	7.54	38.7	6.4
Sn	2911.80	8.42	40.5	7.1
Sb	3025.88	9.37	43.2	7.7

terms must be measured. Since it is important to be consistent with the idea of complete relaxation of the core-hole states, and since our uncorrected $3d$ binding energies are consistent with the literature,[51] we employed M_4 binding energies determined when line-shape asymmetries are removed.[52] In a previous paper,[14] we used uncorrected M_4 energies. The effect of the asymmetry on the Auger parameter, however, is very small.

In Table II, we report the Auger kinetic energy of the most intense experimental peak (mostly $^1G_4$ in the IC scheme), the M_4-M_5 XPS splittings, and the resulting $L_3M_{4,5}M_{4,5}$ Auger parameter. The L_3-M_5 x-ray energies,[50] and the M_4 binding energy[52] are taken from the literature; we estimate the experimental error in determining the peak position at ± 0.5 eV. For clarity, previously reported values of ξ_{MVV} (Ref. 17) were recalculated with the same $B(M_4)$ and are exhibited.

III. DISCUSSION

The assumption of complete relaxation of core-hole states has very clear consequences for the Auger parameter. Since we are dealing with the "ground state" of the core-hole–metal system, it is natural to calculate the binding energies in Eq. (1) in the density-functional formalism[53,54] as integrals over the corresponding Kohn-Sham energy parameters.[7,54–56] Equation (1) then takes the form[13] in Eq. (3a).

$$\xi_{ijk}=\int_0^1 dn_j[\varepsilon_j(n_j,1)-\varepsilon_j(n_j,0)] , \tag{3a}$$

where $\varepsilon_j(n_j,n_k)$ is the self-consistently determined Kohn-Sham[54] energy parameter as a function of the j and k core-level electron occupations (n_j and n_k, respectively). From the form of the Kohn-Sham equations, ξ_{ijk} can be written,[13,14] as the sum of a core term, ξ^c_{ijk}, and a valence term, ξ^v_{ijk},

$$\xi_{ijk}(z)=\xi^c_{ijk}(z)+\xi^v_{ijk}(z) , \tag{3b}$$

$$\xi^m_{ijk}(z)=\int_0^1 dn_j\xi^m_{ijk}(z,n_j) \quad (m=c \text{ or } v) . \tag{3c}$$

The valence term is given by Eq. (3d),[13]

$$\xi^v_{ijk}(z,n_j)=N_j^{-1}\int d^3r\int d^3x\ \psi_j^*(n_j,1;\mathbf{r})\psi_j(n_j,0;\mathbf{r}) \times\{\rho_v(n_j,1;\mathbf{x})-\rho_v(n_j,0;\mathbf{x})\} \times|\mathbf{r}-\mathbf{x}|^{-1} , \tag{3d}$$

$$N_j\equiv\int d^3r\ \ \psi_j^*(n_j,1;\mathbf{r})\psi_j(n_j,0;\mathbf{r}) . \tag{3e}$$

In Eq. (3d), $\psi_j(n_j,n_k;\mathbf{r})$ denotes the self-consistent j core-level solution of the Kohn-Sham equations[54] for the given core-level occupancy and $\rho_v(n_j,n_k;\mathbf{r})$ is the self-consistent valence-electron density, including the screening charge of the core holes[2] (we use atomic units $|e|=\hbar=m=1$), as in Eq. (3f).

$$\rho_v(n_j,n_k;\mathbf{x})\equiv\sum_v n_v(n_j,n_k)|\psi_v(n_j,n_k;\mathbf{x})|^2 . \tag{3f}$$

In Eq. (3f), the sum is over all occupied valence levels and the valence occupancy n_v and wave function ψ_v are written explicitly in terms of the core-level occupations.

Since ρ_v varies slowly on the spatial scale of the core wave functions, we can make the usual, good approximation,[2,44] and write ξ^v_{ijk} as the difference of electrostatic potentials evaluated at the nucleus, which is approximately independent of the explicit final-state core-level identifies. Denoting ξ^v_{ijk} as ξ_v, we have

$$\xi_v(z,n_j)\cong\int d^3x[\rho_v(n_j,1;\mathbf{x})-\rho_v(n_j,0;\mathbf{x})]x^{-1} . \tag{3g}$$

The principal effects of the core holes on ξ_v are twofold: that of modifying the valence wave functions and pulling initially unoccupied states below the Fermi energy and that of attracting screening electrons to these states.[2] These effects are interrelated. The valence wave functions in Eqs. (3) depend directly on the core-hole occupation through the field of the additional positive core-hole charge and indirectly through the additional screening electron charge.

The core-hole contribution is defined in Eq. (4).

$$\xi^c_{ijk}(z,n_j)=N_j^{-1}\int d^3r\int d^3x\ \psi_j^*(n_j,1;\mathbf{r})\psi_j(n_j,0;\mathbf{r})[\{[\rho_c(n_j,1;\mathbf{x})-\rho_c(n_j,0;\mathbf{x})]/|\mathbf{r}-\mathbf{x}|\} +\{V_{xc}(\rho(n_j,1;\mathbf{x}))-V_{xc}(\rho(n_j,0;\mathbf{x}))\}] . \tag{4}$$

The quantity V_{xc} represents the exchange-correlation potential energy, ρ_c denotes the core electron density in exact analogy with Eq. (3f), and $\rho=\rho_c+\rho_v$ is the total electron density. Since the core electrons are spatially localized, $\rho\simeq\rho_c$ in the integral, so that ξ^c_{ijk} depends, to a good approximation, only on core electron properties. In contrast to ξ_v, however, it involves the detailed spatial dependence of the j core wave functions and, so, is not independent of the identity of the final-state core holes.

We can exploit Slater's argument that the valence electrons, being much more delocalized than the core electrons, affect the energy of these states, but do not influence the form of the core electron wave functions.[44] We expect, therefore, ξ^c_{ijk} to be insensitive to the particular valence-electron configuration and to vary slowly as a function of z.

As a consequence of these considerations, we can write ξ_{ijk} as the sum of a slowly varying core term ξ^c_{ijk} which depends on the final-state core-level identities, and a term ξ_v which is sensitive to the valence configuration,[13,14]

$$\xi_{ijk}(z)=\xi^c_{ijk}(z)+\xi_v(z)\ . \tag{5}$$

Our arguments up to this point made no use of the QAM and depended only on the differing spatial variations of the valence and core electrons. Since our arguments were rather general, we expect Eq. (5) to have a wide range of validity. Of course, we should point out that the derivation did depend on a possibly arbitrary separation into core and valence electrons and on the local density approximation[53] for V_{xc}.

The form of Eq. (5) should be valid for any Auger transition involving only core levels. Since ξ_v is independent of exactly which core levels enter the transition under these conditions, the *difference* between the Auger parameters for any two such processes should involve only the difference between the core contributions and, so, should vary slowly as a function of z.

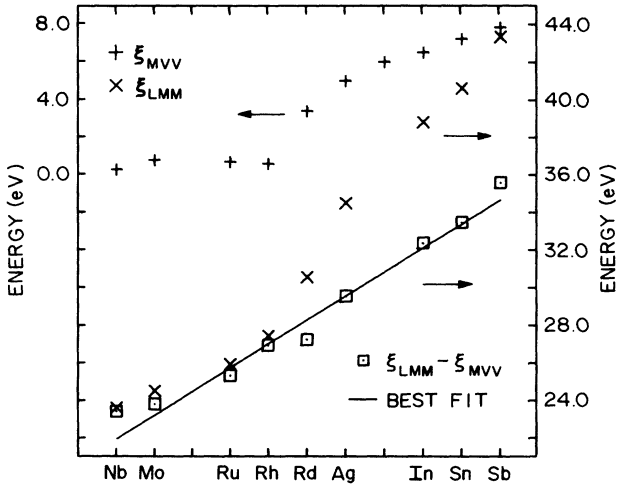

FIG. 2. The Auger parameters for the $M_5N_{4,5}N_{4,5}$ (pluses, from Ref. 17) and the $L_3M_{4,5}M_{4,5}$ (crosses) transitions of the 4*d* metals, as presented in Table II. Also displayed is the difference between them, $\xi_{LMM}-\xi_{MVV}$ (squares), as well as the best linear fit to this difference (i.e., $y=1.269z-30.0322$). It appears that the difference varies approximately linearly, as it should if it involved the difference in core contributions in Eq. (5). The horizontal arrows indicate the ordinate energy scales to be used.

In Fig. 2, we present the individual $L_3M_{4,5}M_{4,5}$ and M_5VV Auger parameters, as well as the difference $\xi_{LMM}-\xi_{MVV}$ between them for the 4*d* metals examined. It is well to note that, although the individual ξ_{ijk} manifest significant jumps as the *d* band becomes filled, the difference varies much more slowly, in accordance with our argument. To emphasize this point further, we display a line which is least-squares fit to the difference (excluding Nb and Pd) under the constraint that it pass through the experimental point for $z=50$. Either relaxation of this constraint or inclusion of Nb and Pd changes the fit little.

In order to proceed further, we make use of a model presented earlier[13,14,38] which applies the excited-atom version of the QAM (Refs. 4 and 7) and the equivalent-core model.[9–12] In this model, the screening electrons are assumed to accommodate themselves self-consistently in the region of the ion so that Eq. (3g) takes the form of Eqs. (6):

$$\xi_v(z,n_j)\cong\sum_\nu\{n_\nu(z+1-n_j)U_\nu(z+1-n_j)-n_\nu(z+2-n_j)U_\nu(z+2-n_j)\}\ , \tag{6a}$$

$$U_\nu(Z_{\rm eff})=\int d^3r|\psi_\nu(Z_{\rm eff};\mathbf{r})|^2r^{-1}\ , \tag{6b}$$

where the sum is over *d* and conduction valence electrons (i.e., $\nu=d$ or *s*), the integral in Eq. (6b) involves the locale of the ionized atom and we consider the core holes as additional protons. The valence occupations $n_\nu(Z_{\rm eff})$ and effective Coulomb integrals $U_\nu(Z_{\rm eff})$ are self-consistent quantities corresponding to the given equivalent core charge,[13,38] $Z_{\rm eff}\equiv z+2-n_j-n_k$ (for the sake of simplicity, we assume that the *s*- and *p*-electron Coulomb integrals are equal, since their spatial extensions are similar[35]). Assuming preferential filling of the *d* states and constant conduction electron occupation when the ground-state *d* bands are unfilled [such that $n_d(Z_{\rm eff})+n_s(Z_{\rm eff})=\text{valence}+2-n_j-n_k$] and a linear variation of the U_ν [i.e., $U_\nu(z+x)=U_\nu(z)+x\Delta U_\nu$, with ΔU_ν constant], we derive Eqs. (7):[9]

$$\xi_v(z)=\xi_v(z_0)-2(z-z_0)\Delta U_s+\Delta\xi_{\rm val}(z)\ , \tag{7a}$$

where z_0 is the atomic number of a reference *sp* metal (we choose Sn in our 4*d* studies). For *sp* metals, $\xi_v(z)$ has a simple form, as in Eq. (7b):

$$\xi_v(z)=\xi_v^{ns}(z)-U_s(z+2)\ , \tag{7b}$$

$$\xi_v^{ns}(z)\equiv-n_d(z)\Delta U_d-n_s(z)\Delta U_s\ , \tag{7c}$$

where $n_d(z)$ and $n_s(z)$ are the ground-state occupations; for *sp* metals, $n_d(z)=10$, $n_s(z)=z-z_{\rm nob}+1$, and $z>z_{\rm nob}$, where we define $z_{\rm nob}$ as the noble-metal atomic number for the series under study. The quantity $\xi_v^{ns}(z)$ is the valence contribution if we neglect the screening response to the core holes and just consider the wave-function dependence.

The first two terms in Eq. (7a) equal the *sp* result in Eqs. (7b) and (7c) extended to general z. The term

$\Delta\xi_{\rm val}(z)$, therefore, represents the difference in screening from that of the *sp* electrons: for *sp* metals, $\Delta\xi_{\rm val}(z)=0.0$. For $z<z_{\rm nob}-1$.

$$\Delta\xi_{\rm val}(z)=-U_{ds}(z_{\rm nob})+[p_{\rm nob}-2(1+z-z_{\rm nob})]\Delta U_{ds}\ , \tag{7d}$$

where we assume that $n_d(z)=10-p_{\rm nob}+(z-z_{\rm nob})$ and $n_s(z)=1+p_{\rm nob}$ for $z\le z_{\rm nob}$ and $p_{\rm nob}$ is the number of ground-state noble-metal *d*-band holes. The quantities $U_{ds}(z_{\rm nob})$ and ΔU_{ds} are defined as $U_{ds}(z_{\rm nob})\equiv U_d(z_{\rm nob})-U_s(z_{\rm nob})$ and $\Delta U_{ds}\equiv\Delta U_d-\Delta U_s$. The variation is linear for the forms of $\Delta\xi_{\rm val}(z)$ in Eqs. (7b) and (7d) because the nature of the screening electrons does not change between the initial and final states [i.e., it is purely *c* type in Eq. (7b) and *d* type in Eq. (7d)]. When the *d* band becomes full during the screening process, however, as for either $z=z_{\rm nob}-1$ [i.e., in the $n_k=0$ term in Eq. (6a)] or $z=z_{\rm nob}$ (in the $n_k=1$ term), the expression is more complicated. For $z=z_{\rm nob}-1$, we have Eq. (7e),

$$\Delta\xi_{\rm val}(z)=-(1-f^2/2)U_{ds}(z_{\rm nob})+[p_{\rm nob}+f^2(3-f)/6]\Delta U_{ds}\ , \tag{7e}$$

where $f\equiv 1-p_{\rm nob}$. The expression for $\Delta\xi_{\rm val}(z)$ when $z=z_{\rm nob}$ is

$$\Delta\xi_{\rm val}(z)=-[(p_{\rm nob}^2)/2]U_{ds}(z_{\rm nob})-[(p_{\rm nob}^3)/6]\Delta U_{ds}\ . \tag{7f}$$

The model described by Eqs. (7), although simple, appears to have sufficient physical content to describe available data. We present, in Fig. 3, the results of calculations and comparison with experimental measurements[13] of the $M_4N_{6,7}N_{6,7}$ transition in the 5*d* series. The term ξ_{MNN} [curve (a)] in the figure corresponds to Eq. (5). The screened valence term [curve (b)] denotes the negative of ξ_v computed from Eq. (7a), whereas the unscreened valence term [curve (c)] represents the negative of ξ_v^{ns} from Eq. (7c). These quantities were calculated with $p_{\rm nob}=0.4$ and Au parameters employed in studies[35] of AuMg and AuZn electronic structure:[57] $U_d({\rm Au})=12.9$ eV, $U_s({\rm Au})=8.38$ eV, $\Delta U_d=1.90$ eV, and $\Delta U_s=1.62$ eV. The core term [curve (d)] is ξ_{MNN}^c from Eq. (7a) and is derived by adjusting the theoretical ξ_{MNN} to the experimental data for $z>79$ [i.e., $\xi_{MNN}(z)=\xi_{MNN}^c(z)+\xi_v(z_0)-2(z-z_0)\Delta U_s$, with $z_0=82$ for Pb] and extrapolating linearly to lower *z*.

Because of our procedure for determining ξ_{MNN}^c, it is really the difference, outside the *sp* region, between the experimental data and the linear extrapolation of the *sp* measurements which is important and with which the theoretical results must agree. This experimentally measured deviation coincides with our definition of $\Delta\xi_{\rm val}$ in Eq. (7a). It is, therefore, clear from Eqs. (7d)–(7f) that the agreement of ξ_{MNN} with experiment shown in Fig. 3 is determined by the parameters $U_{ds}({\rm Au})$ (4.5 eV), ΔU_{ds} (0.28 eV), and $p_{\rm nob}$ and not by the individual effective Coulomb integrals, whose values seem more uncertain.[35]

The dependence on the explicit type of screening electron is displayed in the screened valence term [curve (b)] in Fig. 3. It is interesting to note the linear dependence of $|\xi_v|$ on *z* from Ta through Ir (slope $2\Delta U_d$, reflecting *d*-electron screening) and from Hg through Pb (slope $2\Delta U_s$, reflecting *sp*-electron screening) and the breaks at Pt and at Au. These breaks represent the change from *d*- to *sp*-type screening as the *d* band becomes filled in the two-hole state [i.e., the second term in Eq. 6(a)] in the case of Pt and in the one-hole state [the first term in Eq. 6(a)] in the case of Au. From the figure, it is clear that the valence contribution is nondecreasing throughout the whole range. In this model, the observed jump in the Auger parameter data occurs because the rate of increase of $|\xi_v|$ slows for Pt and Au and cannot compensate the linear increase in the core contribution.

In contrast to the behavior of $|\xi_v|$, the unscreened valence term $|\xi_v^{ns}|$ [curve (c)] in Fig. 3 manifests an almost linear behavior through the whole range of *z*: the slope from Ta to Au is ΔU_d and that from Hg to Pb is ΔU_s. There is a slight break at Au because of its not quite full *d* band [$n_d({\rm Au})=10-p_{\rm nob}=9.6$ electrons/atom].

The derived values of the core term [curve (d)] depend upon our choice of the individual $U_v({\rm Au})$ and ΔU_v [i.e., the sum in Eq. (5) is constrained by the *sp*-metal data]. Although its definition in Eq. (4) involves self-consistent core quantities in the presence of core holes, so that ξ_{MNN}^c is in no way a Slater integral, we may test whether the magnitudes of the core term are reasonable by neglecting the core-hole dependence in Eq. (4) and by averaging over

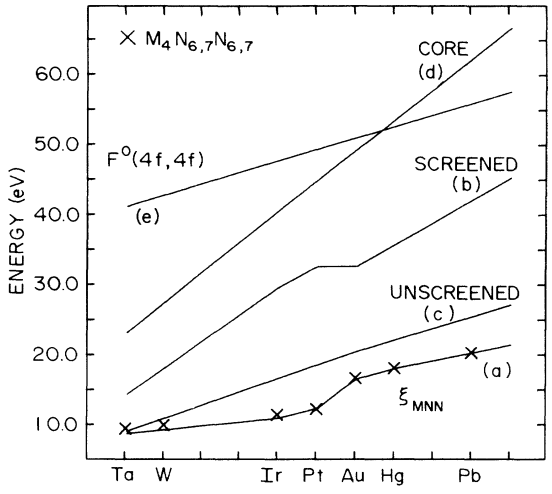

FIG. 3. Curve (a) illustrates the 5*d* metal theoretical Auger parameter in Eq. (5); experimental values for the $M_4N_{6,7}N_{6,7}$ transition are indicated by crosses. Curve (b) represents absolute value of the valence contribution including screening, ξ_v, as calculated from Eqs. (7) with parameters from Refs. 35 and 57: $U_d({\rm Au})=12.9$ eV, $U_s({\rm Au})=8.38$ eV, $\Delta U_d=1.90$ eV, $\Delta U_s=1.62$ eV, and $p_{\rm nob}=0.4$. The absolute value of the corresponding unscreened term ξ_v^{ns} from Eq. (7c) is displayed in curve (c). The core term ξ_{MNN}^c of Eq. (5) as extracted from the data for $z\ge 80$ and extrapolated linearly, is given by curve (d). For comparison, the Slater integral $F^0(4f,4f)$ from Ref. 45 is exhibited in curve (e).

all orbital magnetic quantum numbers of the $4f$ states participating. Averaging in this way yields $F^0(4f,4f)$,[44] whose values we take from Mann's tables[45] and display in curve (e) of Fig. 3. Although F^0 and the core term are not equal, it is interesting that they are of the same order of magnitude. Because of the considerable uncertainty in determining the correct values of the individual effective Coulomb integrals to be used in this and other applications,[35] independent theoretical computations of this quantity would be interesting.

We should point out that the agreement displayed in Fig. 3 [i.e., curve (a)] is intended to demonstrate that the systematics of our model reflects the physical processes governing the experiments. Because of the above-mentioned ambiguity in the choice of effective Coulomb integrals,[35] however, it appears to be more meaningful to compare directly with data in which the core contribution has been removed.[14] One way of removing this contribution is by computing $\Delta\xi_{\rm val}^{\rm expt}$, the deviation of the data from the linear extrapolation of the *sp*-metal Auger parameters,[14]

$$\Delta\xi_{\rm val}^{\rm expt}(z)\equiv\xi_{ijk}(z)-\xi_{ijk}(z_0)-(z-z_0)S\ , \tag{8}$$

where all the quantities on the right-hand side of Eq. (8) are experimental and S denotes the slope of the data in the region of the *sp* metals.[58] The quantity $\Delta\xi_{\rm val}^{\rm expt}$ corresponds exactly to the theoretical quantity $\Delta\xi_{\rm val}$ in Eqs. (7) under the assumption that the core term varies linearly. Note that the interpretation of $\Delta\xi_{\rm val}^{\rm expt}$ as a valence-electron quantity through its definition in Eq. (8) is independent of the details of our model. It really depends on the validity of the separation into core and valence contributions in Eq. (5), on the slowly varying nature of the core contribution, and on the linearity of the valence contribution in the *sp*-metal region. This last assumption seems justified because of the linear response nature of the QAM and of our model[38] and because of the similar spatial properties of the *s* and *p* electrons for the *sp* metals.[35]

In Fig. 4(a), we present $\Delta\xi_{\rm val}^{\rm expt}$ and $\Delta\xi_{\rm val}$ for the $5d$ metals. The reference metal is Pb and $S=1.10$ eV. The agreement manifested is really a reflection of that presented in curve (a) of Fig. 3: that is, the increase in d-electron screening as z increases for $z<78$ is manifest, as is the change from d- to *sp*-type screening as the d band fills for Pt and Au. The important point here is that these quantities involve only the valence-electron contributions and the ambiguities regarding the core contribution have been removed.

The valence contribution to the $4d$ Auger parameter data presented in Table II and Fig. 2 can also be extracted.[14] Because the rate of increase for the $L_3M_{4,5}M_{4,5}$ measurements is rather large in the *sp*-metal region ($z>47$), a small error in determining the slope can have exaggerated consequences when the *sp*-metal data are extrapolated. Since the M_5VV data have a small slope in this region, we exploit the $\xi_{LMM}-\xi_{MVV}$ data in Fig. 2 by employing the linear fit displayed and combining it with the slope of the linear fit to the ξ_{MVV} data in this region (i.e., $z_0=50$). This procedure yields $S=1.874$ eV for the

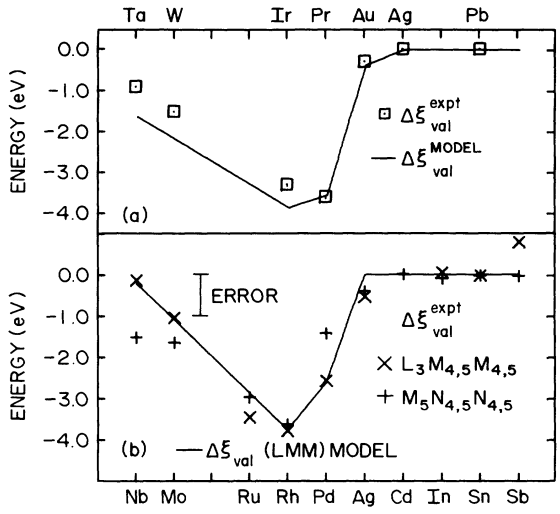

FIG. 4. (a) The solid line represents the theoretical valence quantity $\Delta\xi_{\rm val}(z)$ calculated from Eqs. (7) with the same parameters used in curve (a) of Fig. 3. The squares symbolize the experimental quantity $\Delta\xi_{\rm val}^{\rm expt}(z)$ derived from the data in Fig. 3 through Eq. (8), with $S=1.10$ eV. (b) The crosses and pluses represent $\Delta\xi_{\rm val}^{\rm expt}(z)$ for the $L_3M_{4,5}M_{4,5}$ and $M_5N_{4,5}N_{4,5}$ Auger transitions, respectively, calculated from Eq. (8) with $S=1.874$ and 0.605 eV, respectively. The solid line illustrates the consistency of the model when the parameters are extracted from the $L_3M_{4,5}M_{4,5}$ data: $U_{ds}({\rm Ag})=4.69$ eV, $\Delta U_{ds}=0.445$ eV, and $p_{\rm nob}=0.1$

$L_3M_{4,5}M_{4,5}$ measurements and $S=0.605$ for the $M_5N_{4,5}N_{4,5}$ data.

The results for $\Delta\xi_{\rm val}^{\rm expt}$ for the $L_3M_{4,5}M_{4,5}$ and $M_5N_{4,5}N_{4,5}$ Auger parameters are exhibited in Fig. 4(b). The agreement between the two sets of data within experimental error (±0.5 eV) indicates that, except possibly for Nb and Pd, the d-band holes appear to behave like core holes.[59]

The similarity between the $5d$ and $4d$ measurements suggests the possibility of extracting the model parameters from the data by employing Eqs. (7) for $\Delta\xi_{\rm val}$. A reasonable procedure is that of determining $U_{ds}({\rm Ag})$ and ΔU_{ds} in the region where the ground-state d band has more than two holes (i.e., $z\leq45$) and then determining $p_{\rm nob}$ from least-squares fitting the Pd and Ag data, with which the model should be consistent. In Fig. 4(b), we present the results for $\Delta\xi_{\rm val}$ (i.e., the solid line) from this procedure, where the model was constrained to be equal to the $L_3M_{4,5}M_{4,5}$ data for Rh: the corresponding parameters are $U_{ds}({\rm Ag})=4.69$ eV, $\Delta U_{ds}=0.445$ eV, and $p_{\rm nob}=0.1$. This value of $p_{\rm nob}$ for Ag is insensitive to the exact procedure we use and is in reasonable agreement with band-structure calculations.[60,61]

Applying this procedure to the $M_5N_{4,5}N_{4,5}$ measurements yields the same degree of agreement and $U_{ds}({\rm Ag})=4.26$ eV, $\Delta U_{ds}=0.289$ eV, and $p_{\rm nob}=0.0$, with the same degree of insensitivity to procedure. This value of $p_{\rm nob}$, however, represents a best value, but not a true minimum of the least-squares fit. Although the agree-

ment is reasonable, therefore, it is not really clear whether the Pd measurement is consistent with the rest of the data within the context of this model: that is, it is not clear whether the d-band holes in Pd are corelike.

Disregarding our reservations concerning the Pd M_5VV data, it seems that both sets of data are consistent with the model. The parameters vary between, say, 4.0 and 5.0 eV for U_{ds}(Ag), between 0.27 and 0.49 eV for ΔU_{ds}, and between 0.0 and 0.1 for $p_{\rm nob}$. Such uncertainty in the parameters is not unreasonable, considering the experimental errors and the simplicity of the model. A value of 4.1 eV for U_{ds}(Ag) was derived from renormalized atom calculations.[60]

One more comment on the model is appropriate. The assumption that $U_v(z)$ is linear, with a constant slope, appears to be justified as long as the nature of the screening electrons does not change between the one-hole and two-hole states. For the 4d series, therefore, the screening electrons are purely sp type for $z>47$ and purely d type for $z<46$ and the assumption is reasonable.[38] For either $z=46$ or 47, however, the nature of the screening electron changes, and one expects the slope of $U_v(z)$ to change, since it is a valence quantity.[38] The agreement between the model results and the data suggests that this effect is minor.

IV. CONCLUSIONS

In this paper, we present the results of measurements of the $L_3M_{4,5}M_{4,5}$ Auger transition in the 4d metals. The spectra, as exemplified by In in Fig. 1, are well described in an intermediate-coupling representation. Measurements of the peak energies permit determination of the Auger parameters shown in Fig. 2.

By exploiting the idea of complete screening of the core holes, we show that the measured Auger parameter of transitions involving only core levels can be written as the sum of a slowly varying core contribution and a valence term which is sensitive to the valence configuration and insensitive to the core levels involved. We test this result by subtracting the Auger parameters of the $L_3M_{4,5}M_{4,5}$ and previously reported[17] $M_5N_{4,5}N_{4,5}$ transitions. The ensuing difference in Fig. 2 does, indeed, appear to vary linearly, as it should if it were the difference in core terms.

Application of a model based on the quasiatomic picture and the equivalent-core model permits determination of the separate contributions to the Auger parameter, which we illustrate for the 5d series in Fig. 3. Although the derived values for the core contribution appear reasonable, uncertainties in the effective Coulomb integrals produce ambiguities in the extracted core terms.

The general systematics of the model allows for subtraction of the effects of the core contribution by exploiting measurements for the sp metals. The resulting valence quantity, $\Delta\xi_{\rm val}^{\rm expt}$, is defined experimentally in Eq. (8) and we present the results for the 5d and 4d series in Figs. 4(a) and 4(b), respectively. The corresponding theoretical quantity, $\Delta\xi_{\rm val}$, defined in Eqs. (7), involves only the differences in d- and sp-electron effective Coulomb integrals, which appear to be less uncertain than the individual quantities themselves.[35]

The similarity in $\Delta\xi_{\rm val}^{\rm expt}$ in Fig. 4(b) for the $L_3M_{4,5}M_{4,5}$ and $M_5N_{4,5}N_{4,5}$ transitions of the 4d metals indicates that the valence-electron screening processes are similar in the two cases, except possibly for Pd and Nb: that is to say, the d-band holes appear to behave like core holes in so far as the valence screening is concerned.

Extraction of the relevant screening parameters from the model results in values similar to those for the 5d metals in Fig. 4(a), which explains the similarity in appearance between the 4d and 5d results. In particular, the $L_3M_{4,5}M_{4,5}$ data for Pd and Ag appear to require, for the sake of consistency, that the number of d-band holes in Ag be approximately 0.1, which agrees with band-structure results.[60,61] The difference in effective Coulomb integrals derived is reasonably consistent with renormalized atom results.[60]

In summary, then, it appears possible to unambiguously extract the valence screening contribution to the measured Auger parameter by exploiting the systematics of the experimental data, and to investigate the nature of the screening process by exploiting the quasiatomic model. Results for most of the 4d metals (except possibly Pd) indicate that the d-band holes behave as though they have core nature.

ACKNOWLEDGMENTS

We would like to thank R. C. G. Vinhas and R. F. Suarez for technical assistance. This work was supported by CNPq, FAPESP, and FINEP of Brazil. P. A. P. Nascente thanks FAPESP for support.

[1]B. Johansson and N. Mårtensson, Phys. Rev. B **21**, 4427 (1980).
[2]N. D. Lang and A. R. Williams, Phys. Rev. B **16**, 2408 (1977).
[3]G. G. Kleiman, Appl. Surf. Sci. **11/12**, 730 (1982).
[4]A. R. Williams, and N. D. Lang, Phys. Rev. Lett. **40**, 954 (1978).
[5]N. Mårtensson and B. Johansson, Phys. Rev. Lett. **45**, 482 (1980).
[6]N. Mårtensson, R. Nyholm, and B. Johansson, Phys. Rev. Lett. **45**, 754 (1980).
[7]N. D. Lang and A. R. Williams, Phys. Rev. B **20**, 1369 (1979).
[8]N. Mårtensson, P. Hedegård, and B. Johansson, Phys. Scr. **29**, 154 (1984).
[9]L. Ley, S. P. Kowalczyk, F. R. McFeely, R. A. Pollack, and D. A. Shirley, Phys. Rev. B **8**, 2392 (1973).
[10]D. A. Shirley, R. L. Martin, S. P. Kowalczyk, F. R. McFeely, and L. Ley, Phys. Rev. B **15**, 544 (1977).
[11]S. P. Kowalczyk, R. A. Pollack, F. R. McFeely, L. Ley, and D. A. Shirley, Phys. Rev. B **8**, 2387 (1973).
[12]S. P. Kowalczyk, L. Ley, F. R. McFeely, R. A. Pollack, and D. A. Shirley, Phys. Rev. B **9**, 381 (1974).
[13]G. G. Kleiman, S. G. C. de Castro, J. D. Rogers, and V. S. Sundaram, Solid State Commun. **43**, 257 (1982).
[14]G. G. Kleiman, R. Landers, S. G. C. de Castro, and P. A. P. Nascente, Phys. Rev. B **44**, 3383 (1991); J. Vac. Sci. Technol.

A (to be published).
[15]J. D. Rogers, V. S. Sundaram, G. G. Kleiman, S. G. C. de Castro, R. A. Douglas, and A. C. Peterlevitz, J. Phys. F **12**, 2097 (1982).
[16]E. Antonides, E. C. Janse, and G. A. Sawatzky, Phys. Rev. B **15**, 1669 (1977).
[17]N. Mårtensson and R. Nyholm, Phys. Rev. B **24**, 7121 (1981).
[18]R. Nyholm, K. Helenelund, B. Johansson, and S. Hórnstróm, Phys. Rev. B **34**, 675 (1986).
[19]Auger parameters of the $N_{6,7}O_{4,5}O_{4,5}$ (i.e., $N_{6,7}VV$) transition in the 5*d* series (Ref. 18) seem to exhibit a jump between Ir and Pt and not between Pt and Au, in contrast to the 3*d* and 4*d* series. This is attributed to the much larger band influence in the 5*d* metals even though Au and Pt seem to have strong quasiatomic components (Ref. 18).
[20]M. Iwan, F. J. Himpsel, and D. E. Eastman, Phys. Rev. Lett. **43**, 1829 (1979).
[21]M. Iwan, E. E. Koch, T. C. Chiang, and F. J. Himpsel, Phys. Lett. **76A**, 177 (1980).
[22]G. A. Sawatzky, Phys. Rev. Lett. **39**, 504 (1977).
[23]M. Cini, Solid State Commun. **20**, 605 (1976); **24**, 681 (1977); Phys. Rev. B **17**, 2728 (1978).
[24]P. Weightman, P. T. Andrews, and A. C. Parry-Jones, J. Phys. C **12**, 3635 (1979).
[25]M. Vos, D. v. d. Marel, and G. A. Sawatzky, Phys. Rev. B **29**, 3073 (1984).
[26]M. Vos, G. A. Sawatzky, M. Davies, P. Weightman, and P. T. Andrews, Solid State Commun. **52**, 159 (1984).
[27]P. Hedegård and B. Johansson, Phys. Rev. B **31**, 7749 (1985); Phys. Rev. Lett. **52**, 2168 (1984).
[28]M. Vos, D. van der Marel, G. A. Sawatzky, M. Davies, P. Weightman, and P. T. Andrews, Phys. Rev. Lett. **54**, 1334 (1985).
[29]P. Hedegård and B. Johansson, Phys. Rev. Lett. **54**, 1335 (1985).
[30]G. G. Kleiman, R. Landers, S. G. C. de Castro, and P. A. P. Nascente, Phys. Rev. B **45**, 13 899 (1992).
[31]P. Weightman and P. T. Andrews, J. Phys. C **13**, L821 (1980).
[32]P. Weightman, P. T. Andrews, G. M. Stocks, and H. Winter, J. Phys. C **16**, L81 (1983).
[33]M. Davies and P. Weightman, J. Phys. C **17**, L1015 (1984).
[34]P. Weightman, H. Wright, S. D. Waddington, D. van der Marel, G. A. Sawatzky, G. P. Diakun, and D. Norman, Phys. Rev. B **36**, 9098 (1987).
[35]T. D. Thomas and P. Weightman, Phys. Rev. B **33**, 5406 (1986).
[36]J. C. Fuggle, in *Electron Spectroscopy,* edited by C. R. Brundle and A. D. Baker (Academic, London, 1981), Vol. 4.
[37]P. A. P. Nascente, S. G. C. de Castro, R. Landers, and G. G. Kleiman, Phys. Rev. B **43**, 4659 (1991).
[38]G. G. Kleiman, R. Landers, S. G. C. de Castro, and J. D. Rogers, Phys. Rev. B **4**, 8529 (1991).
[39]N. Mårtensson, R. Nyholm, H. Calên, J. Hedman, and B. Johansson, Phys. Rev. B **24**, 1725 (1981).
[40]V. S. Sundaram, J. D. Rogers, and R. Landers, J. Vac. Sci. Technol. **19**, 117 (1981).
[41]D. A. Shirley, Phys. Rev. B **5**, 4709 (1972).
[42]M. P. Seah and W. A. Dench, Surf. Interface Anal. **1**, 2 (1979).
[43]E. U. Condon and G. H. Shortley, *The Theory of Atomic Spectra* (Cambridge University, London, 1963).
[44]J. C. Slater, *Quantum Theory of Atomic Structure* (McGraw-Hill, New York, 1960), Vol. 2.
[45]J. B. Mann, Los Alamos Scientific Laboratory Report No. LASL-3690 (unpublished).
[46]J. F. McGilp, P. Weightman, and E. J. McGuire, J. Phys. C **10**, 3445 (1977).
[47]E. J. McGuire, in *Atomic Inner-Shell Processes,* edited by B. Crasemann (Academic, London, 1975).
[48]E. J. McGuire, Sandia Laboratory Report No. SC-RR-710075, 1971 (unpublished).
[49]G. G. Kleiman, R. Landers, P. A. P. Nascente, and S. G. C. de Castro, Phys. Rev. B **46**, 1970 (1992).
[50]J. A. Bearden, Rev. Mod. Phys. **39**, 78 (1967).
[51]R. Nyholm and N. Mårtensson, J. Phys. C **13**, L279 (1980).
[52]R. Nyholm and N. Mårtensson, Solid State Commun. **40**, 311 (1981).
[53]P. Hohenberg and W. Kohn, Phys. Rev. **136**, B864 (1964).
[54]W. Kohn and L. J. Sham, Phys. Rev. **140**, A1133 (1965).
[55]J. F. Janak, Phys. Rev. B **18**, 7165 (1978).
[56]Such a procedure is strictly valid only for the true ground state. The justification is largely empirical.
[57]The values of U_s(Au), ΔU_d, and ΔU_s employed in the text were taken directly from Ref. 35. That for U_d(Au) was derived by scaling the corresponding free-atom value, 12.21 eV, of Ref. 35 by a factor of 1.24/1.17 corresponding to a "solid-state" correction of the free-atom value of $\langle 1/r \rangle$. This procedure produces a value of 4.5 eV for U_d(Au)$-U_s$(Au), which is larger than the values from Ref. 35. Direct use of parameters from Ref. 35 yields agreement with experiment of the same quality as that in Fig. 3.
[58]In Ref. 14, the factor of 2*S* in the expression corresponding to Eq. (8) should be written *S*.
[59]In Ref. 14, the experimental slope for either transition was approximated by ξ_{ijk}(Sn)$-\xi_{ijk}$(In), which changes the values of $\Delta\xi_{\rm val}^{\rm expt}$ somewhat, especially for the $L_3M_{4,5}M_{4,5}$ transition. Nevertheless, the conclusions remain unchanged.
[60]C. D. Gelatt, Jr. and H. Ehrenreich, Phys. Rev. B **10**, 398 (1974).
[61]F. M. Mueller, Phys. Rev. **153**, 659 (1967).